

Multiparameter Quantum Metrology of Incoherent Point Sources: Towards Realistic Superresolution

J. Řehaček,¹ Z. Hradil,¹ B. Stoklasa,¹ M. Paúr,¹ J. Grover,² A. Krzic,² and L. L. Sánchez-Soto^{3,4}

¹*Department of Optics, Palacký University, 17. listopadu 12, 771 46 Olomouc, Czech Republic*

²*ESA—Advanced Concepts and Studies Office, European Space Research Technology Centre (ESTEC), Keplerlaan 1, Postbus 299, NL-2200AG Noordwijk, Netherlands*

³*Departamento de Óptica, Facultad de Física, Universidad Complutense, 28040 Madrid, Spain*

⁴*Max-Planck-Institut für die Physik des Lichts, Günther-Scharowsky-Straße 1, Bau 24, 91058 Erlangen, Germany*

We establish the multiparameter quantum Cramér-Rao bound for simultaneously estimating the centroid, the separation, and the relative intensities of two incoherent optical point sources using a linear imaging system. For equally bright sources, the Cramér-Rao bound is independent of the source separation, which confirms that the Rayleigh resolution limit is just an artifact of the conventional direct imaging and can be overcome with an adequate strategy. For the general case of unequally bright sources, the amount of information one can gain about the separation falls to zero, but we show that there is always a quadratic improvement in an optimal detection in comparison with the intensity measurements. This advantage can be of utmost important in realistic scenarios, such as observational astronomy.

The time-honored Rayleigh criterion [1] specifies the minimum separation between two incoherent optical sources using a linear imaging system. As a matter of fact, it is the size of the point spread function [2] that determines the resolution: two points closer than the PSF width will be difficult to resolve due to the substantial overlap of their images.

Thus far, this Rayleigh criterion has been considered as a fundamental limit. Resolution can only be improved either by reducing the wavelength or by building higher numerical-aperture optics, thereby making the PSF narrower. Nonetheless, outstanding methods have been developed lately that can break the Rayleigh limit under special circumstances [3–12]. Though promising, these techniques are involved and require careful control of the source, which is not always possible, especially in astronomical applications.

Despite being very intuitive, the common derivation of the Rayleigh limit is heuristic and it is deeply rooted in classical optical technology [13]. Recently, inspired by ideas of quantum information, Tsang and coworkers [14–17] have revisited this problem using the Fisher information and the associated Cramér-Rao lower bound (CRLB) to quantify how well the separation between two point sources can be estimated. When only the intensity at the image is measured (the basis of all the conventional techniques), the Fisher information falls to zero as the separation between the sources decreases and the CRLB diverges accordingly; this is known as the Rayleigh curse [14]. However, when the Fisher information of the complete field is calculated, it stays constant and so does the CRLB, revealing that the Rayleigh limit is not essential to the problem.

These remarkable predictions prompted a series of experimental implementations [18–20] and further generalizations [21–25], including the related question of source localization [26–28]. All this previous work has focused on the estimation of the separation, taking for granted a highly symmetric configuration with identical sources. In this Letter, we approach the issue in a more realistic scenario, where both sources may have unequal intensities. This involves the simultaneous estimation of separation, centroid, and intensi-

ties. Typically, when estimating multiple parameters, there is a trade-off in how well different parameters may be estimated: when the estimation protocol is optimized from the point of view of one parameter, the precision with which the remaining ones can be estimated deteriorates.

Here, we show that including intensity in the estimation problem does lead to a reduction in the information for unbalanced sources. However the information available in an optimal measurement still surpasses that of a conventional direct imaging scheme by a significant margin at small separations. This suggests possible applications, for example, in observational astronomy, where sources typically have small angular separations and can have large differences in brightness.

Let us first set the stage for our simple model. We assume quasimonochromatic paraxial waves with one specified polarization and one spatial dimension, x denoting the image-plane coordinate. The corresponding object-plane coordinates can be obtained via the lateral magnification of the system, which we take to be linear spatially invariant [2].

To facilitate possible generalizations, we phrase what follows in a quantum parlance. A wave of complex amplitude $U(x)$ can thus be assigned to a ket $|U\rangle$, such that $U(x) = \langle x|U\rangle$, where $|x\rangle$ is a vector describing a point-like source at x .

The system is characterized by its PSF, which represents its normalized intensity response to a point source. We denote this PSF by $I(x) = |\langle x|\Psi\rangle|^2 = |\Psi(x)|^2$, so that $\Psi(x)$ can be interpreted as the amplitude PSF.

Two incoherent point sources, of different intensities and separated by a distance \mathfrak{s} , are imaged by that system. The signal can be represented as a density operator

$$\rho_{\theta} = q\rho_{+} + (1-q)\rho_{-}, \quad (1)$$

where q and $1-q$ are the intensities of the sources, with the proviso that the total intensity is normalized to unity. In addition, we have defined $\rho_{\pm} = |\Psi_{\pm}\rangle\langle\Psi_{\pm}|$ and the x -displaced PSF states are

$$\langle x|\Psi_{\pm}\rangle = \langle x - \mathfrak{s}_0 \mp \mathfrak{s}/2|\Psi\rangle = \Psi(x - \mathfrak{s}_0 \mp \mathfrak{s}/2), \quad (2)$$

so that they are symmetrically located around the geometric centroid $\mathfrak{s}_0 = \frac{1}{2}(x_+ + x_-)$. Note that

$$|\Psi_{\pm}\rangle = \exp[-i(\mathfrak{s}_0 \pm \mathfrak{s}/2)P]|\Psi\rangle, \quad (3)$$

where P is the momentum operator, which generates displacements in the x variable. As in quantum mechanics, it acts as a derivative $P = -i\partial_x$. These spatial modes are not orthogonal ($\langle\Psi_-|\Psi_+\rangle \neq 0$), so they cannot be separated by independent measurements.

The density matrix ρ_{θ} gives the normalized mean intensity: $\rho_{\theta}(x) = q|\Psi(x - \mathfrak{s}_0 - \mathfrak{s}/2)|^2 + (1 - q)|\Psi(x - \mathfrak{s}_0 + \mathfrak{s}/2)|^2$, and depends on the centroid \mathfrak{s}_0 , the separation \mathfrak{s} , and the relative intensities of the sources q . This is indicated by the vector $\theta = (\mathfrak{s}_0, \mathfrak{s}, q)^t$. The task is to estimate the values of θ through the measurement of some observables on ρ_{θ} . In turn, a quantum estimator $\hat{\theta}$ for θ is a selfadjoint operator representing a proper measurement followed by data processing performed on the outcomes. Such a parameter estimation implies an additional uncertainty for the measured value, which cannot be avoided.

In this multiparameter estimation scenario, the central quantity is the quantum Fisher information matrix (QFIM) [29]. This is a natural generalization of the classical Fisher information, which is a mathematical measure of the sensitivity of an observable quantity (the PSF, in our case) to changes in its underlying parameters. However, the QFIM is optimized over all the possible quantum measurements. It is defined as

$$Q_{\alpha\beta}(\theta) = \frac{1}{2} \text{Tr}(\rho_{\theta} \{L_{\alpha}, L_{\beta}\}), \quad (4)$$

where the Greek indices run over the components of the vector θ and $\{\cdot, \cdot\}$ denotes the anticommutator. Here, L_{α} stands for the symmetric logarithmic derivative [30] with respect to the parameter θ_{α} , defined implicitly by $\frac{1}{2}(L_{\alpha}\rho_{\theta} + \rho_{\theta}L_{\alpha}) = \partial_{\alpha}\rho_{\theta}$, with $\partial_{\alpha} = \partial/\partial\theta_{\alpha}$.

Upon writing ρ_{θ} in its eigenbasis $\rho_{\theta} = \sum_n \lambda_n |\lambda_n\rangle\langle\lambda_n|$, the QFIM per detection event can be concisely expressed as [31]

$$Q_{\alpha\beta}(\theta) = 2 \sum_{m,n} \frac{1}{\lambda_m + \lambda_n} \langle\lambda_m|\partial_{\alpha}\rho_{\theta}|\lambda_n\rangle\langle\lambda_n|\partial_{\beta}\rho_{\theta}|\lambda_m\rangle, \quad (5)$$

and the summation extends over m, n with $\lambda_m + \lambda_n \neq 0$. In addition, the constraints of unity trace $\sum_m \lambda_m = 1$ and the completeness relation $\sum_m |\lambda_m\rangle\langle\lambda_m| = \mathbb{1}$ have to be imposed.

The QFIM is a distinguishability metric on the space of quantum states and leads to the multiparameter quantum CRLB [32, 33]:

$$\text{Cov}(\hat{\theta}) \geq Q^{-1}(\theta), \quad (6)$$

where $\text{Cov}(\hat{\theta}) = \mathbb{E}[(\hat{\theta}_{\alpha} - \theta_{\alpha})(\hat{\theta}_{\beta} - \theta_{\beta})]$ refers to the covariance matrix for a locally unbiased estimator $\hat{\theta}$ of the quantity θ and $\mathbb{E}[Y]$ is the expectation value of the random variable Y . In particular, the individual parameter θ_{α} can be estimated

with a variance satisfying $\text{Var}(\hat{\theta}_{\alpha}) \geq (Q^{-1})_{\alpha\alpha}(\theta)$, and a positive operator-valued measurement (POVM) attaining this accuracy is given by the eigenvectors of L_{α} . Unlike for a single parameter, the collective bound is not always saturable: the intuitive reason for this is incompatibility of the optimal measurements for different parameters [34].

If the operators L_{α} corresponding to the different parameters commute, there is no additional difficulty in extracting maximal information from a state on all parameters simultaneously. If they do not commute, however, this does not immediately imply that it is impossible to simultaneously extract information on all parameters with precision matching that of the separate scenario for each. As discussed in a number of papers [35–37] the multiparameter quantum CRLB can be saturated provided

$$\text{Tr}(\rho_{\theta}[L_{\alpha}, L_{\beta}]) = 0. \quad (7)$$

Then, optimal measurements can be found by optimizing over the classical Fisher information, as the QFIM is an upper bound for the former quantity. This can be efficiently accomplished by global optimization algorithms [38]. For our particular case, it is easy to see that the condition (7) is fulfilled whenever the PSF is real, $\Psi(x)^* = \Psi(x)$, which will be assumed henceforth.

To proceed further, we note that the density matrix ρ_{θ} is, by definition, of rank 2. The QFIM reduces then to the simpler form

$$\begin{aligned} Q_{\alpha\beta} = & -\frac{3}{\lambda_1} \langle\lambda_1|\partial_{\alpha}\rho_{\theta}|\lambda_1\rangle\langle\lambda_1|\partial_{\beta}\rho_{\theta}|\lambda_1\rangle \\ & -\frac{3}{\lambda_2} \langle\lambda_2|\partial_{\alpha}\rho_{\theta}|\lambda_2\rangle\langle\lambda_2|\partial_{\beta}\rho_{\theta}|\lambda_2\rangle \\ & + 4 \left(1 - \frac{1}{\lambda_1} - \frac{1}{\lambda_2}\right) \langle\lambda_1|\partial_{\alpha}\rho_{\theta}|\lambda_2\rangle\langle\lambda_2|\partial_{\beta}\rho_{\theta}|\lambda_1\rangle \\ & + \frac{4}{\lambda_1} \langle\lambda_1|\partial_{\alpha}\rho_{\theta}\partial_{\beta}\rho_{\theta}|\lambda_1\rangle + \frac{4}{\lambda_2} \langle\lambda_2|\partial_{\alpha}\rho_{\theta}\partial_{\beta}\rho_{\theta}|\lambda_2\rangle. \end{aligned} \quad (8)$$

The derivatives involved in this equation can be easily evaluated; the result reads

$$\begin{aligned} \partial_{\mathfrak{s}_0}\rho_{\theta} &= i[\rho_{\theta}, P], \\ \partial_{\mathfrak{s}}\rho_{\theta} &= \frac{i}{2}(q[\rho_+, P] - (1-q)[\rho_-, P]), \\ \partial_q\rho_{\theta} &= \rho_+ - \rho_-. \end{aligned} \quad (9)$$

To complete the calculation it proves convenient to write the two nontrivial eigenstates of ρ_{θ} in terms of non-orthogonal component states $|\Psi_{\pm}\rangle$: $|\lambda_{1,2}\rangle = a_{1,2}|\Psi_+\rangle + b_{1,2}|\Psi_-\rangle$, where $a_{1,2}$ and $b_{1,2}$ are easy-to-find yet complex functions of the separation and the intensities and whose explicit form is of no relevance for our purposes here. Substituting this and Eq. (9) into Eq. (8), and after a lengthy calculation, we obtain a compact expression for the QFIM

$$Q = 4 \begin{pmatrix} p^2 + 4q(1-q)\wp^2 & (q-1/2)p^2 & -i\wp\wp \\ (q-1/2)p^2 & p^2/4 & 0 \\ -i\wp\wp & 0 & \frac{1-w^2}{4q(1-q)} \end{pmatrix}. \quad (10)$$

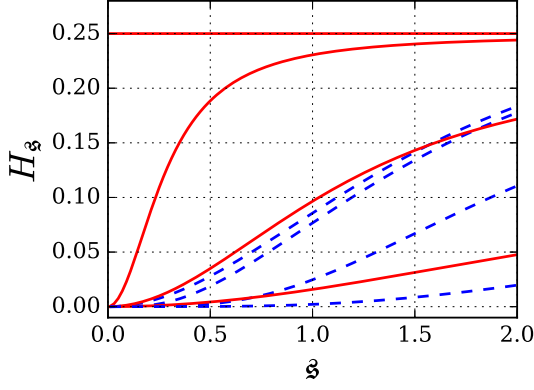


FIG. 1. Precision H_s in the separation s as inferred by optimal (red solid lines) and direct (blue broken lines) detections for different relative intensities of the two sources. The values of q , from top to bottom, are 0.5, 0.45, 0.3, and 0.1. Notice that the performance of the optimal detection is rather sensitive to small deviations from equal brightness over a wide range of separations.

This is our central result. The QFIM depends only on the following quantities

$$\begin{aligned} w &\equiv \langle \Psi_{\pm} | \Psi_{\mp} \rangle = \langle \Psi | \exp(isP) | \Psi \rangle, \\ p^2 &\equiv \langle \Psi_{\pm} | P^2 | \Psi_{\pm} \rangle = \langle \Psi | P^2 | \Psi \rangle, \\ \wp &\equiv \pm \langle \Psi_{\pm} | P | \Psi_{\mp} \rangle = \langle \Psi | \exp(isP) P | \Psi \rangle. \end{aligned} \quad (11)$$

Interestingly, p^2 is fully determined by the shape of the PSF, whereas both w and \wp depend on the separation s . Furthermore, \wp is purely imaginary.

In what follows, rather than the variances themselves, we will use the inverses $H_{\alpha} = 1/\text{Var}(\theta_{\alpha})$, usually called the precisions [39]. In this way, we avoid potential divergences at $s = 0$.

The QFIM (10) nicely shows the interplay between various signal parameters. First, notice that Q is independent of the centroid, as might be expected. Second, for equally bright sources, $q = 1/2$, the measurement of separation s is uncorrelated with the measurements of the remaining parameters and we have $H_s(q = 1/2) = p^2$, a well known result, and the Rayleigh curse is lifted [20]. This happy coincidence does not hold for unequal intensities $q \neq 1/2$; now, the separation is correlated with the centroid (via the intensity term $q - 1/2$) and the centroid is correlated with the intensity (via p^2). This can be intuitively understood: unequal intensities result in asymmetrical images and finding the centroid is no longer a trivial task. This asymmetry, in turn, depends on the relative brightness of the two components. Hence, all the three parameters become entangled and, as we shall see, having separation-independent information about s is no longer possible.

By inverting the QFIM we immediately get

$$H_s = p^2 \frac{\mathcal{Q}^2 \wp^2 + \mathcal{Q}^2 p^2 (1 - w^2)}{\mathcal{Q}^2 \wp^2 + p^2 (1 - w^2)}, \quad (12)$$

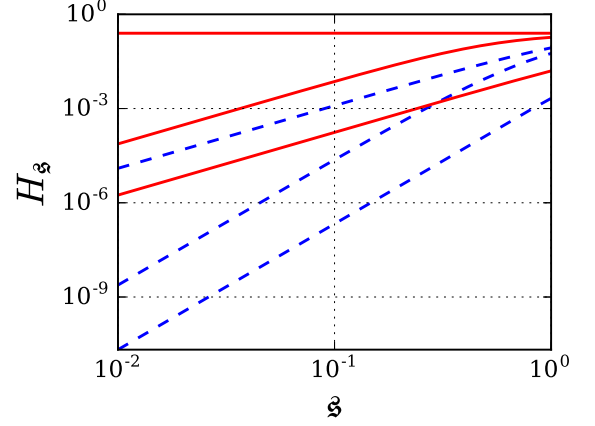


FIG. 2. Precisions as in Fig. 1, but visualized on a logarithmic scale. Slopes of straight lines translate to the powers of s . The values of q are, from top to bottom, 0.5, 0.4, and 0.1.

where $0 \leq \mathcal{Q}^2 \equiv 4q(1 - q) \leq 1$. Obviously, $H_s(q) \leq H_s(q = 1/2) = p^2$ and $\lim_{q \rightarrow 0,1} H_s(q) = 0$, which demonstrates that resolving two highly unequal sources is difficult, even at the quantum limit.

The instance of large brightness differences and small separations is probably the most interesting regime encountered, e. g., in exoplanet observations. We first expand the s -dependent quantities:

$$\begin{aligned} w(s) &= \langle \Psi | e^{isP} | \Psi \rangle \simeq 1 - \frac{1}{2} p^2 s^2 + \frac{1}{24} p^4 s^4, \\ p(s) &= \langle \Psi | P e^{isP} | \Psi \rangle \simeq i p^2 s - i \frac{1}{6} p^4 s^3, \end{aligned} \quad (13)$$

where $p^4 = \langle \Psi | P^4 | \Psi \rangle$ is the fourth moment of the PSF momentum. Then, as $s \ll 1$, we get (for $0 < \mathcal{Q} < 1$)

$$\begin{aligned} H_{s_0} &\simeq \mathcal{Q}^2 \text{Var}(\hat{P}^2) s^2, \\ H_s &\simeq \frac{\mathcal{Q}^2}{4(1 - \mathcal{Q}^2)} \text{Var}(\hat{P}^2) s^2, \\ H_q &\simeq \frac{1}{\mathcal{Q}^2} \text{Var}(\hat{P}^2) s^4. \end{aligned} \quad (14)$$

The PSF enters these expressions through the variance of P^2 : $\text{Var}(\hat{P}^2) = p^4 - p^2$. This leaves room for optimization, provided the PSF can be controlled. For a fixed PSF, the information about all three parameters apparently vanishes with $s \rightarrow 0$ unless $q = 1/2$. And since exactly balanced sources never happen, the information about very small separations always drops to near zero and the Rayleigh curse is unavoidable. However, significant improvements of the optimal measurement schemes over the standard intensity detection are still possible.

To illustrate this point let us consider a Gaussian response $\langle x | \Psi \rangle = (2\pi)^{(1/4)} \exp(-x^2/4)$ of unit width, which will serve from now on as our basic unit length. We shall compare the quantum limit given by (10) with that given by the classical Fisher information for the direct intensity measurement. We assume no prior knowledge about any of the three parameters.

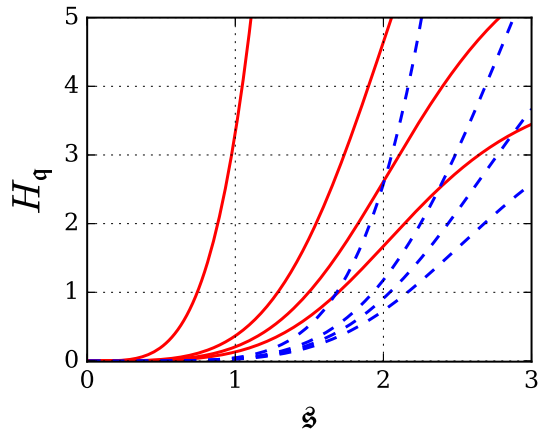


FIG. 3. Precision about relative intensity q as inferred by the optimal detection (red solid lines) and the direct detection (blue broken lines) for different relative intensities of the two sources. The values of q , from bottom to top are 0.5, 0.2, 0.1, and 0.01.

Figure 1 plots information about separation H_s for different relative intensities q . Unbalanced intensities make both optimal and intensity detection go to zero for small separations, however the former at a much slower rate. Hence, optimal information to intensity information increases with decreasing separations, regardless of whether the sources are balanced.

The reason becomes obvious with the same data visualized on the logarithmic scales, as shown in Fig. 2. In the region of $s \ll \sigma$, we can discern two regimes of importance. For balanced sources, $H_s^{\text{opt}} \propto 1$ and $H_s^{\text{int}} \propto s^2$. For unbalanced sources, $H_s^{\text{opt}} \propto s^2$, as we have seen, and $H_s^{\text{int}} \propto s^4$. In consequence, there is always a factor of s^{-2} improvement of the optimal detection over the standard one, irrespective of the true values of the signal parameters. In practice, this means that when we already are well below the Rayleigh limit, if we decrease the separation 10 times, about 10,000 times more photons must be detected with a CCD camera to keep the accuracy of the measurement, while only 100 times more would suffice for optimal measurement. This amounts to saving 99% of detection time with the optimal detection scheme.

Finally, Fig. 3 presents a similar comparison now concerning the information about the relative intensity H_q . Here, optimal information and intensity information always scale as s^4 and s^6 , respectively, and the same s^{-2} gain in performance appears. Notice the reversed ordering of curves with q , meaning that now, the information increases rather than decreases with increasing intensity difference, which reveals the complementarity between these magnitudes. Also notice that the broken lines converge as we approach $s = 0$. It can be shown that the leading term for intensity detection for small separations is p -independent in contrast to the optimal detection, which displays a strong $H_q^{\text{opt}} \propto q^{-1}$ dependence for $q \ll 1/2$. This highlights the advantage of an optimal detection scheme for astronomical observations. For example more than a quarter of catalogued binary systems consist of stars that differ in

brightness by more than an order of magnitude [40], and the darkest known exoplanet is three orders of magnitude dimmer than its host star in the infrared [41].

In summary, we have presented a comprehensive analysis of the ultimate precision bounds for estimating the centroid, the separation, and the relative intensities of two pointlike incoherent sources. For equally bright sources, the quantum Fisher information remains constant, which translates into the fact that the Rayleigh limit is not essential and can be lifted. On the other hand, for unequally bright sources, the information about very small separations always drops to near zero and the Rayleigh curse is unavoidable. Nonetheless, significant improvements can still be expected with optimal detection schemes.

We acknowledge financial support from the Technology Agency of the Czech Republic (Grant TE01020229), the Grant Agency of the Czech Republic (Grant No. 15-03194S), the IGA Project of the Palacký University (Grant No. IGA PrF 2016-005), the European Space Agency's ARIADNA scheme, and the Spanish MINECO (Grant FIS2015-67963-P).

-
- [1] Lord Rayleigh, "Investigations in optics, with special reference to the spectroscope," *Phil. Mag.* **8**, 261–274 (1879).
 - [2] J. W. Goodman, *Introduction to Fourier Optics* (Roberts and Company, Englewood, 2004).
 - [3] A. J. den Dekker and A. van den Bos, "Resolution: a survey," *J. Opt. Soc. Am. A* **14**, 547–557 (1997).
 - [4] E. Betzig, G. H. Patterson, R. Sougrat, O. W. Lindwasser, S. Olenych, J. S. Bonifacino, M. W. Davidson, J. Lippincott-Schwartz, and H. F. Hess, "Imaging intracellular fluorescent proteins at nanometer resolution," *Science* **313**, 1642 (2006).
 - [5] S. T. Hess, T. P. K. Girirajan, and M. D. Mason, "Ultra-high resolution imaging by fluorescence photoactivation localization microscopy," *Biophys. J.* **91**, 4258–4272 (2006).
 - [6] S. W. Hell, "Far-field optical nanoscopy," *Science* **316**, 1153–1158 (2007).
 - [7] M. I. Kolobov, "Quantum Imaging," (Springer, Berlin, 2007) Chap. Quantum Limits of Optical Super-Resolution, pp. 113–138.
 - [8] Focus issue: Super-resolution Imaging, *Nat. Photonics* **3**, 361–420 (2009).
 - [9] S. W. Hell, "Microscopy and its focal switch," *Nat. Meth.* **6**, 24–32 (2009).
 - [10] G. Patterson, M. Davidson, S. Manley, and J. Lippincott-Schwartz, "Superresolution imaging using single-molecule localization," *Annu. Rev. Phys. Chem.* **61**, 345–367 (2010).
 - [11] P. R. Hemmer and T. Zapata, "The universal scaling laws that determine the achievable resolution in different schemes for super-resolution imaging," *J. Opt.* **14**, 083002 (2012).
 - [12] C. Cremer and R. B. Masters, "Resolution enhancement techniques in microscopy," *Eur. Phys. J. H* **38**, 281–344 (2013).
 - [13] E. Abbe, "Ueber einen neuen Beleuchtungsapparat am Mikroskop," *Arch. Mikrosk. Anat.* **9**, 469–480 (1873).
 - [14] M. Tsang, R. Nair, and X.-M. Lu, "Quantum theory of superresolution for two incoherent optical point sources," *Phys. Rev. X* **6**, 031033 (2016).
 - [15] R. Nair and M. Tsang, "Far-field superresolution of thermal electromagnetic sources at the quantum limit,"

- Phys. Rev. Lett. **117**, 190801 (2016).
- [16] S. Z. Ang, R. Nair, and M. Tsang, “Quantum limit for two-dimensional resolution of two incoherent optical point sources,” *Phys. Rev. A* **95**, 063847 (2016).
- [17] M. Tsang, “Subdiffraction incoherent optical imaging via spatial-mode demultiplexing,” *New J. Phys.* **19**, 023054 (2017).
- [18] F. Yang, A. Taschilina, E. S. Moiseev, C. Simon, and A. I. Lvovsky, “Far-field linear optical superresolution via heterodyne detection in a higher-order local oscillator mode,” *Optica* **3**, 1148–1152 (2016).
- [19] W. K. Tham, H. Ferretti, and A. M. Steinberg, “Beating Rayleigh’s curse by imaging using phase information,” *Phys. Rev. Lett.* **118**, 070801 (2016).
- [20] M. Paur, B. Stoklasa, Z. Hradil, L. L. Sanchez-Soto, and J. Rehacek, “Achieving the ultimate optical resolution,” *Optica* **3**, 1144–1147 (2016).
- [21] C. Lupo and S. Pirandola, “Ultimate precision bound of quantum and subwavelength imaging,” *Phys. Rev. Lett.* **117**, 190802 (2016).
- [22] H. Krovi, S. Guha, and J. H. Shapiro, “Attaining the quantum limit of passive imaging,” arXiv:16009.00684 (2016).
- [23] J. Rehacek, M. Pař, B. Stoklasa, Z. Hradil, and L. L. Sánchez-Soto, “Optimal measurements for resolution beyond the rayleigh limit,” *Opt. Lett.* **42**, 231–234 (2017).
- [24] R. Kerviche, S. Guha, and A. Ashok, “Fundamental limit of resolving two point sources limited by an arbitrary point spread function,” in *2017 IEEE International Symposium on Information Theory (ISIT)* (2017) pp. 441–445.
- [25] Q. Zhuang, Z. Zhang, and J. H. Shapiro, “Quantum illumination for enhanced detection of rayleigh-fading targets,” *Phys. Rev. A* **96**, 020302 (2017).
- [26] T. Z. Sheng, K. Durak, and A. Ling, “Fault-tolerant and finite-error localization for point emitters within the diffraction limit,” *Opt. Express* **24**, 22004–22012 (2016).
- [27] M. Tsang, “Quantum limits to optical point-source localization,” *Optica* **2**, 646–653 (2015).
- [28] R. Nair and M. Tsang, “Interferometric superlocalization of two incoherent optical point sources,” *Opt. Express* **24**, 3684–3701 (2016).
- [29] D. Petz and C. Ghinea, “Introduction to Quantum Fisher Information,” in *Quantum Probability and Related Topics*, Vol. Volume 27 (World Scientific, 2011) pp. 261–281.
- [30] C. W. Helstrom, “Minimum mean-squared error of estimates in quantum statistics,” *Phys. Lett. A* **25**, 101–102 (1967).
- [31] M. G. A. Paris, “Quantum estimation for quantum technology,” *Int. J. Quantum Inform.* **07**, 125–137 (2009).
- [32] M. Szczykulska, T. Baumgratz, and A. Datta, “Multi-parameter quantum metrology,” *Adv. Phys.* **1**, 621–639 (2016).
- [33] S. L. Braunstein and C. M. Caves, “Statistical distance and the geometry of quantum states,” *Phys. Rev. Lett.* **72**, 3439–3443 (1994).
- [34] A. S. Holevo, *Probabilistic and Statistical Aspects of Quantum Theory*, 2nd ed. (North Holland, Amsterdam, 2003).
- [35] S. Ragy, M. Jarzyna, and R. Demkowicz-Dobrzański, “Compatibility in multiparameter quantum metrology,” *Phys. Rev. A* **94**, 052108 (2016).
- [36] K. Matsumoto, “A new approach to the Cramér-Rao-type bound of the pure-state model,” *J. Phys. A: Math. Gen.* **35**, 3111 (2002).
- [37] P. J. D. Crowley, A. Datta, M. Barbieri, and I. A. Walmsley, “Tradeoff in simultaneous quantum-limited phase and loss estimation in interferometry,” *Phys. Rev. A* **89**, 023845 (2014).
- [38] R. Horst and P. M. Pardalos, eds., *Handbook of Global Optimization* (Springer, Berlin, 1995).
- [39] J. M. Bernardo and A. F. M. Smith, *Bayesian Theory* (Wiley, Sussex, 2000).
- [40] <http://www.usno.navy.mil/usno/astrometry/optical-ir-prod/wds/dm3>.
- [41] T. Barclay, D. Huber, J. F. Rowe, J. J. Fortney, C. V. Morley, E. V. Quintana, D. C. Fabrycky, G. Barentsen, S. Bloemen, J. L. Christiansen, B.-O. Demory, B. J. Fulton, J. M. Jenkins, F. Mullally, D. Ragozzine, S. E. Seader, A. Shporer, P. Tenenbaum, and S. E. Thompson, “Photometrically derived masses and radii of the planet and star in the tres-2 system,” *Astrophys. J.* **761**, 53 (2012).